Supplementary information for:

Synthesis, X-ray Structure and Electrochemical Properties of Hybrid Binuclear Metallophthalocyaninate-Capped tris-Pyridineoximates

Semyon V. Dudkin[a], Alexander S. Belov[a], Yulia V. Nelyubina[a], Anastasia V. Savchuk[b], Alexander A. Pavlov[a], Valentin V. Novikov[a], and Yan Z. Voloshin[a,c]

[a]*Nesmeyanov Institute of Organoelement Compounds of the Russian Academy of Sciences, 119991, Moscow, Russia*

[b]*Vernadskii Institute of General and Inorganic Chemistry of the National Academy of Sciences of Ukraine, 03680 Kiev, Ukraine*

[c]*Gubkin Russian State University of Oil and Gas, 119991 Moscow, Russia*

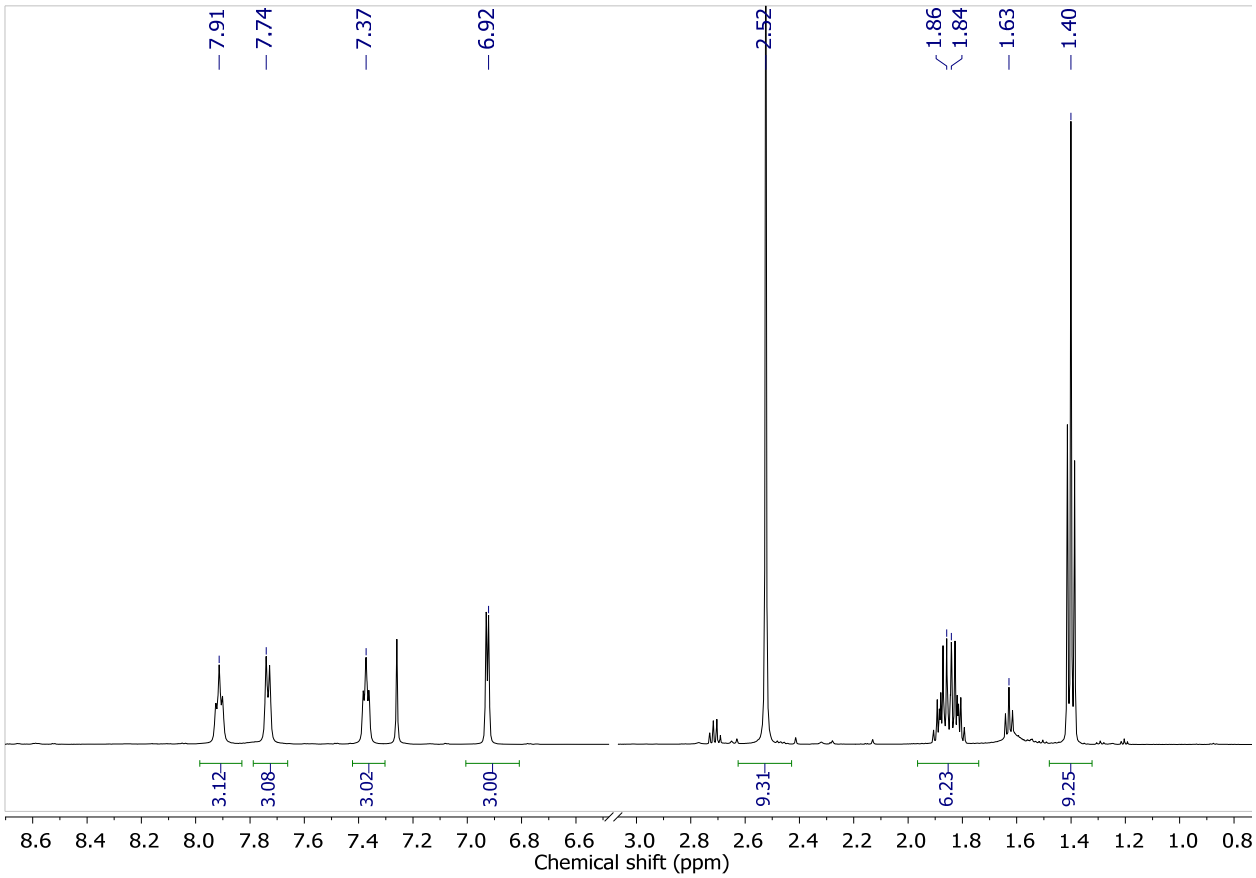

Fig. S1. ^{1}H NMR spectrum of the solution of the complex **[Fe(AcPyOx)$_3$(Sb(C$_2$H$_5$)$_3$)](ClO$_4$)** in $CDCl_3$.

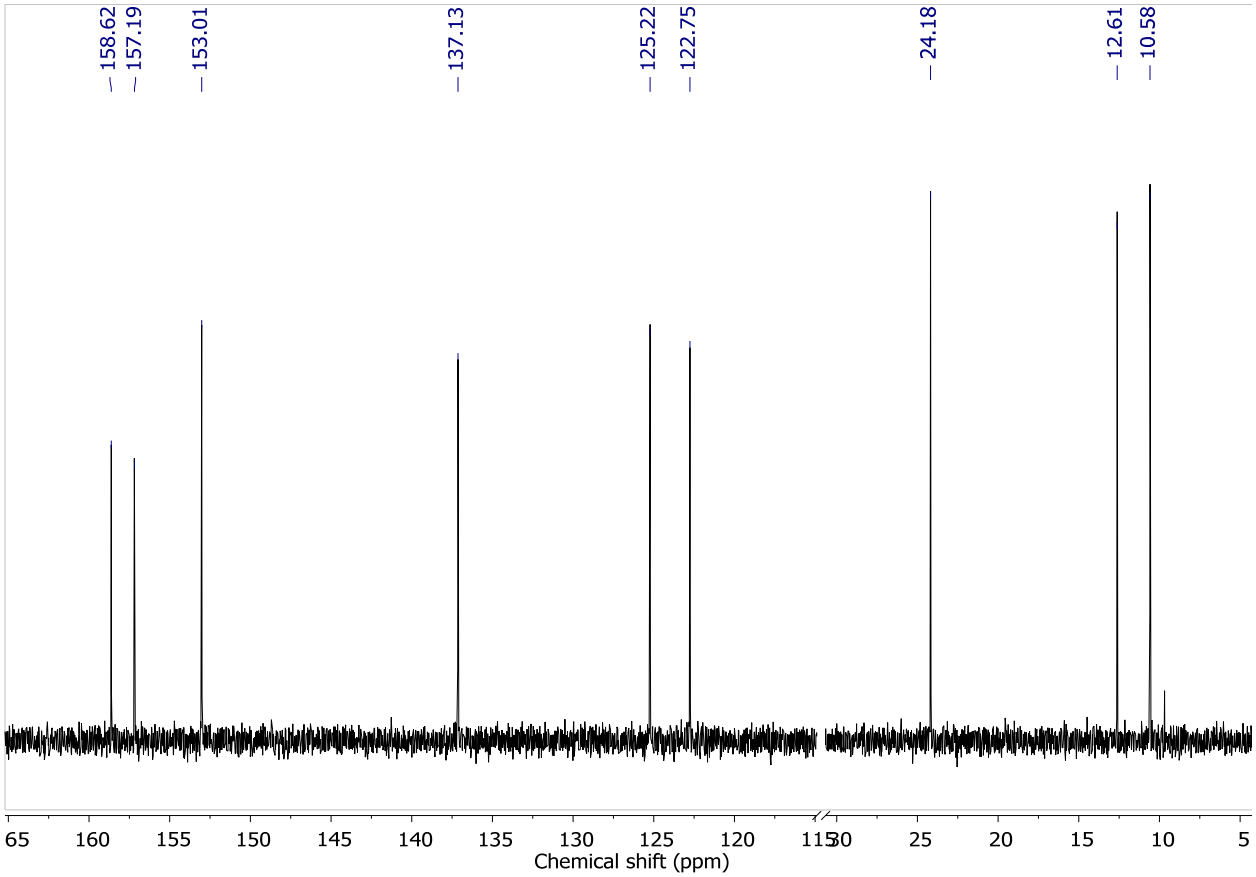

Fig. S2. ^{13}C NMR spectrum of the solution of the complex [**Fe(AcPyOx)$_3$(Sb(C$_2$H$_5$)$_3$)](ClO$_4$)** in $CDCl_3$.

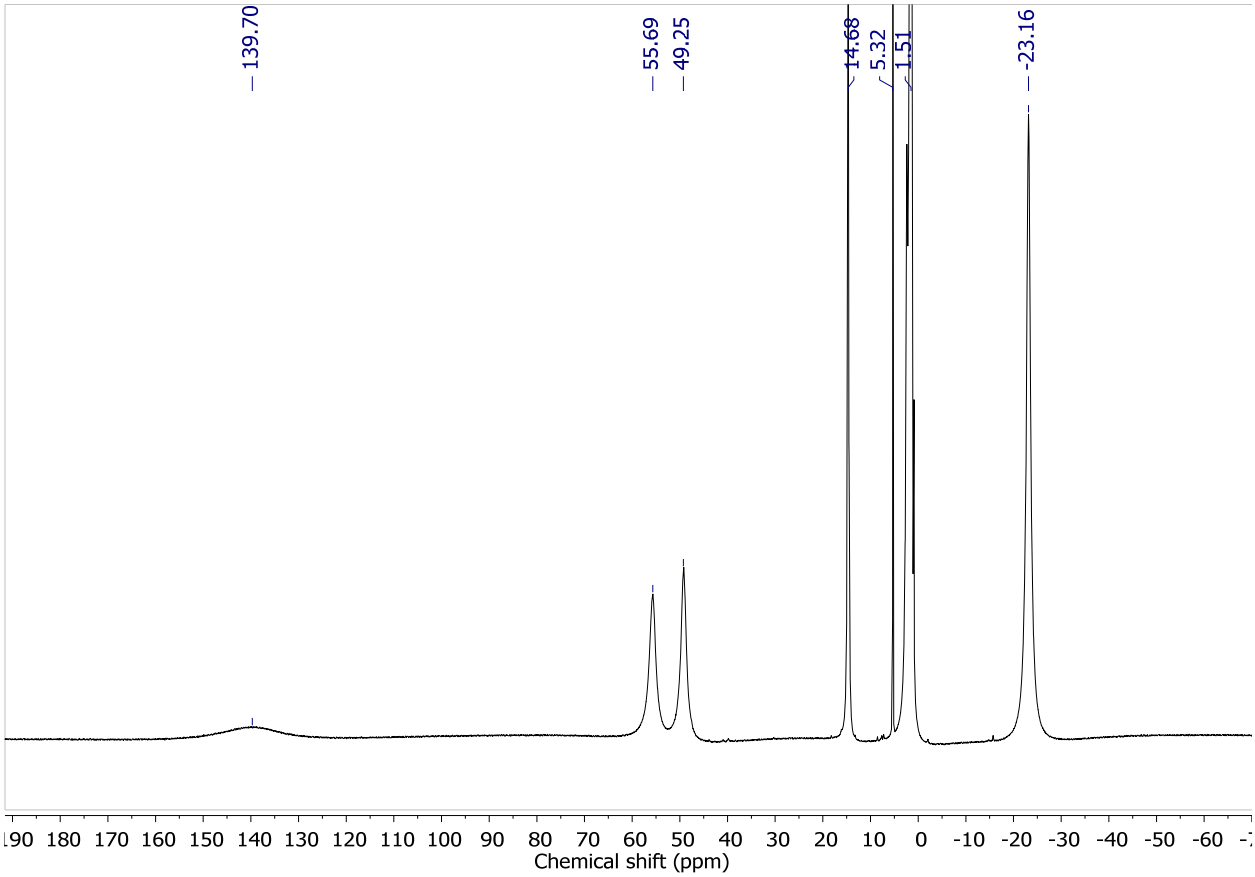

Fig. S3. ^{1}H NMR spectrum of the solution of the complex [**Ni(AcPyOx)$_3$(Sb(C$_2$H$_5$)$_3$)](ClO$_4$)** in CD_2Cl_2.

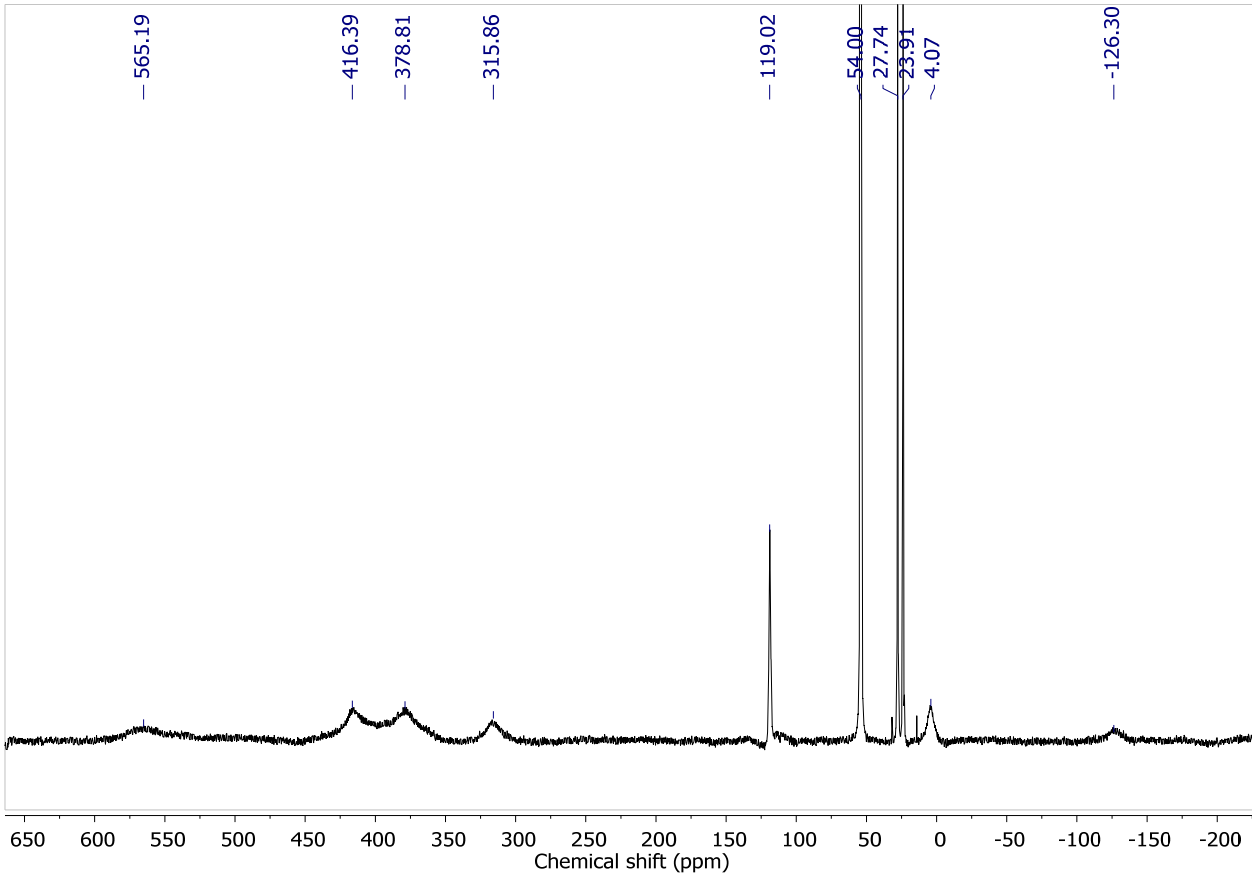

Fig. S4. ^{13}C NMR spectrum of the solution of the complex [**Ni(AcPyOx)$_3$(Sb(C$_2$H$_5$)$_3$)](ClO$_4$)** in CD_2Cl_2.

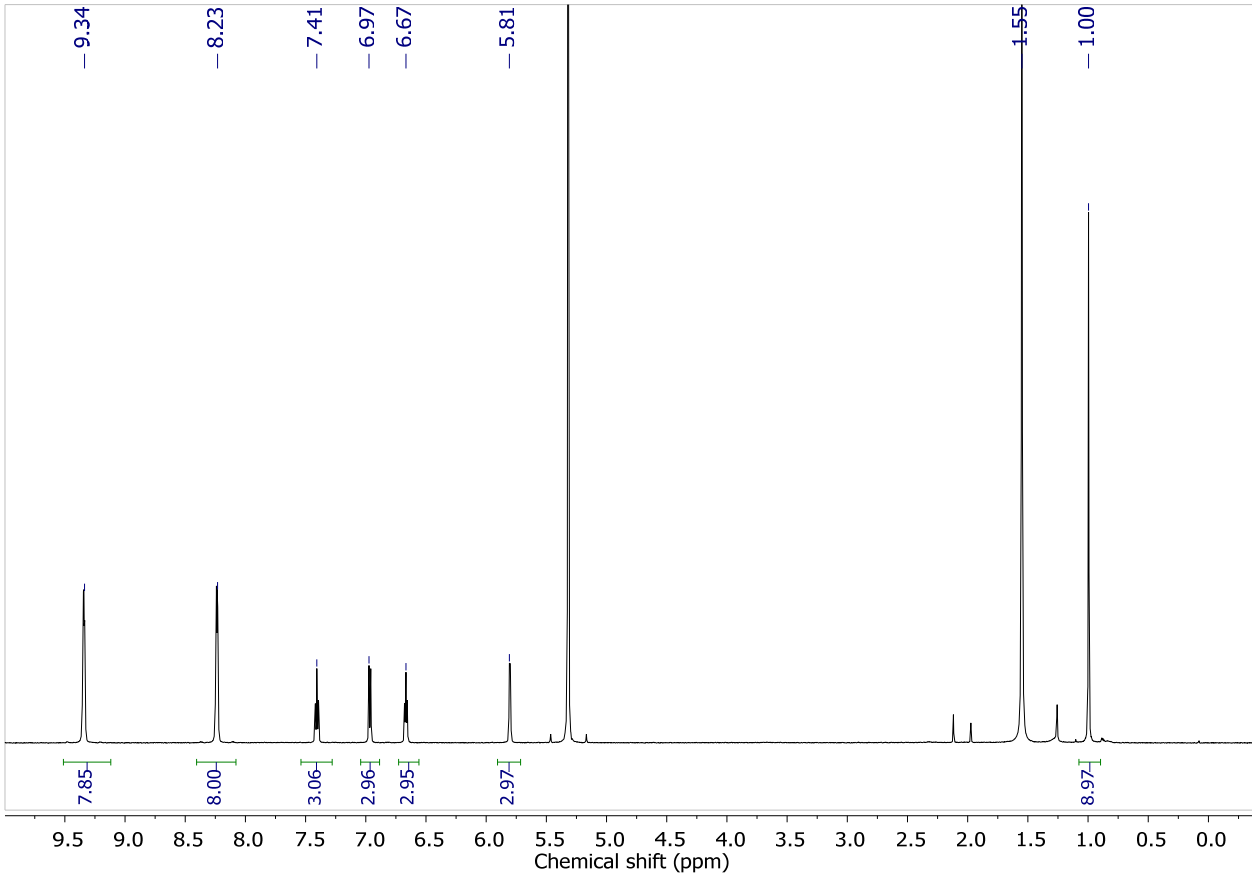

Fig. S5. ^{1}H NMR spectrum of the solution of the complex [**Fe(AcPyOx)$_3$(HfPc)](ClO$_4$)** in CD_2Cl_2.

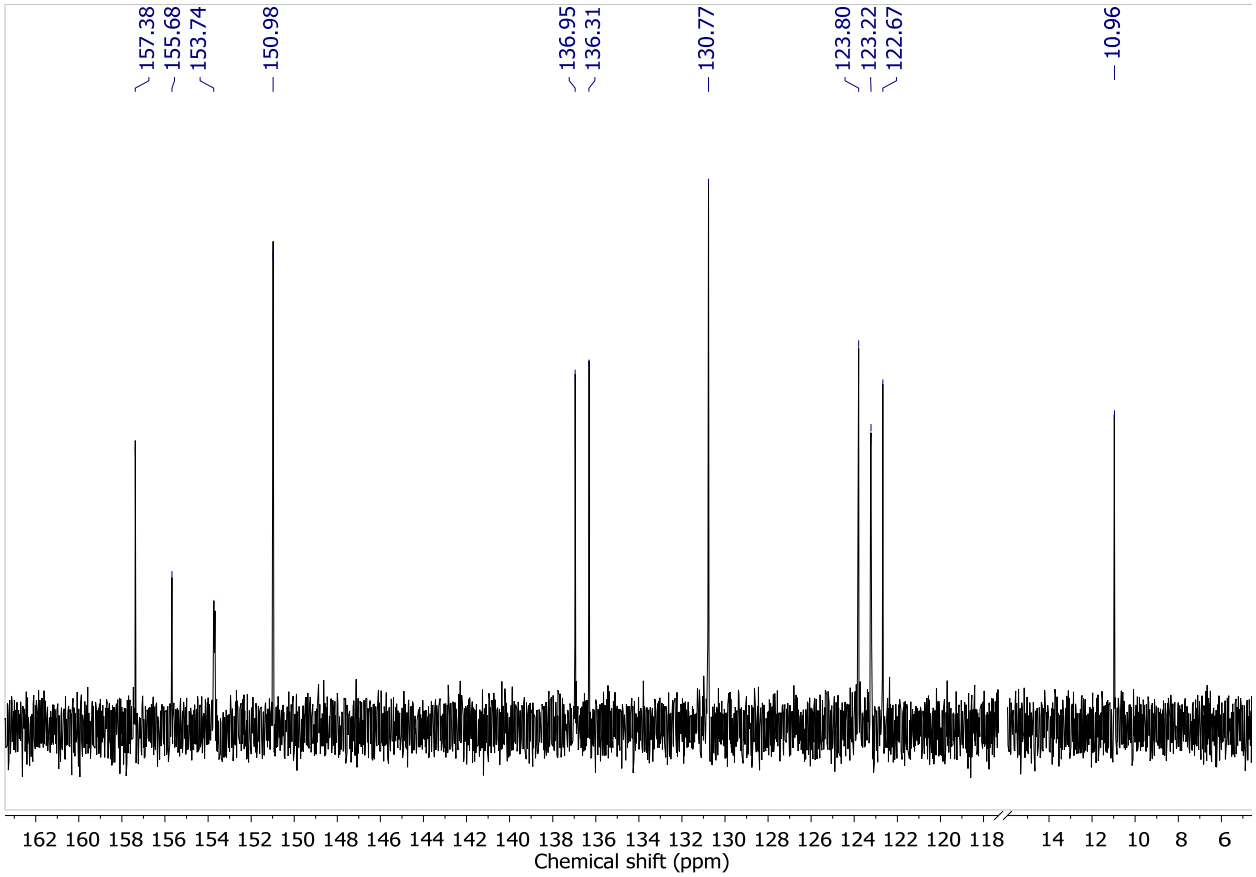

Fig. S6. ^{13}C NMR spectrum of the solution of the complex [**Fe(AcPyOx)$_3$(HfPc)](ClO$_4$)** in CD_2Cl_2.

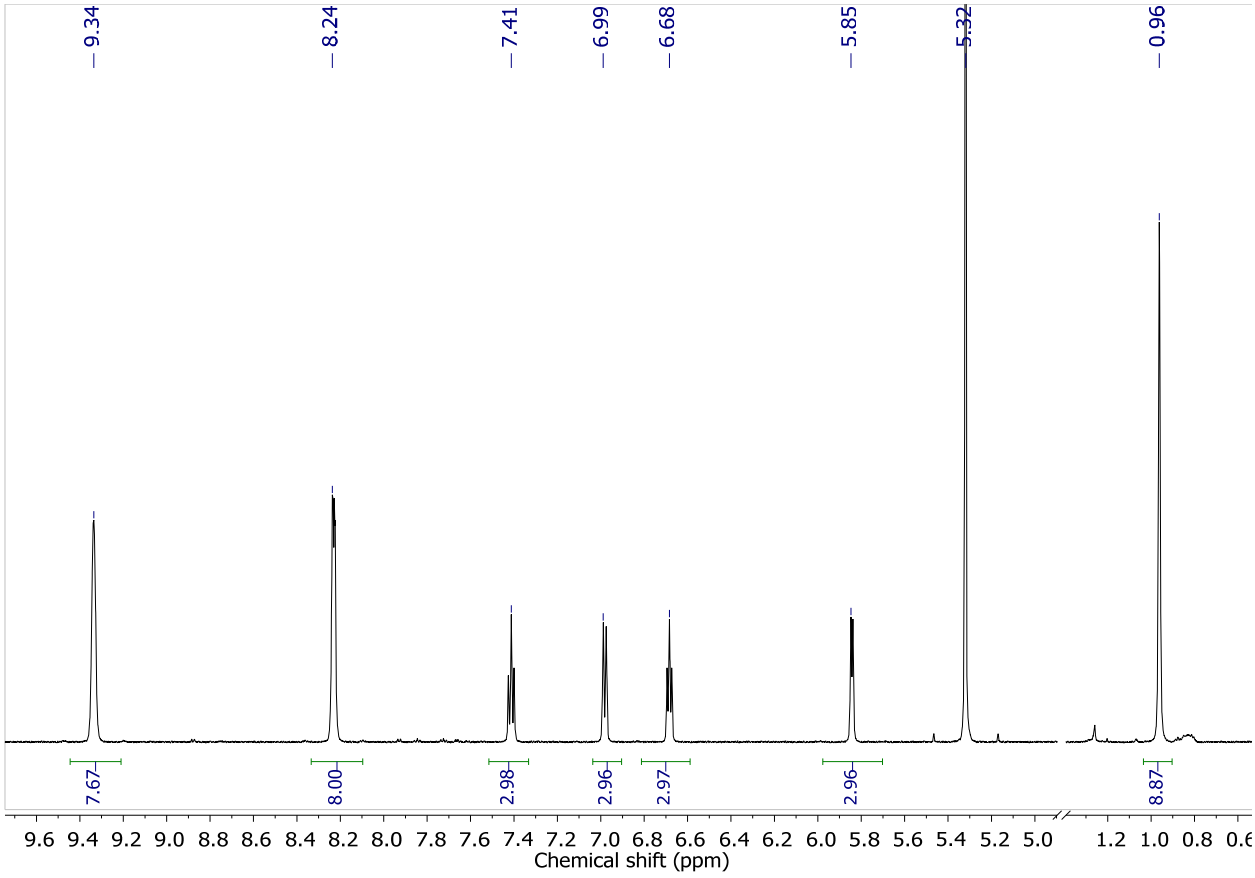

Fig. S7. ^{1}H NMR spectrum of the solution of the complex [**Fe(AcPyOx)$_3$(ZrPc)](ClO$_4$)** in CD_2Cl_2.

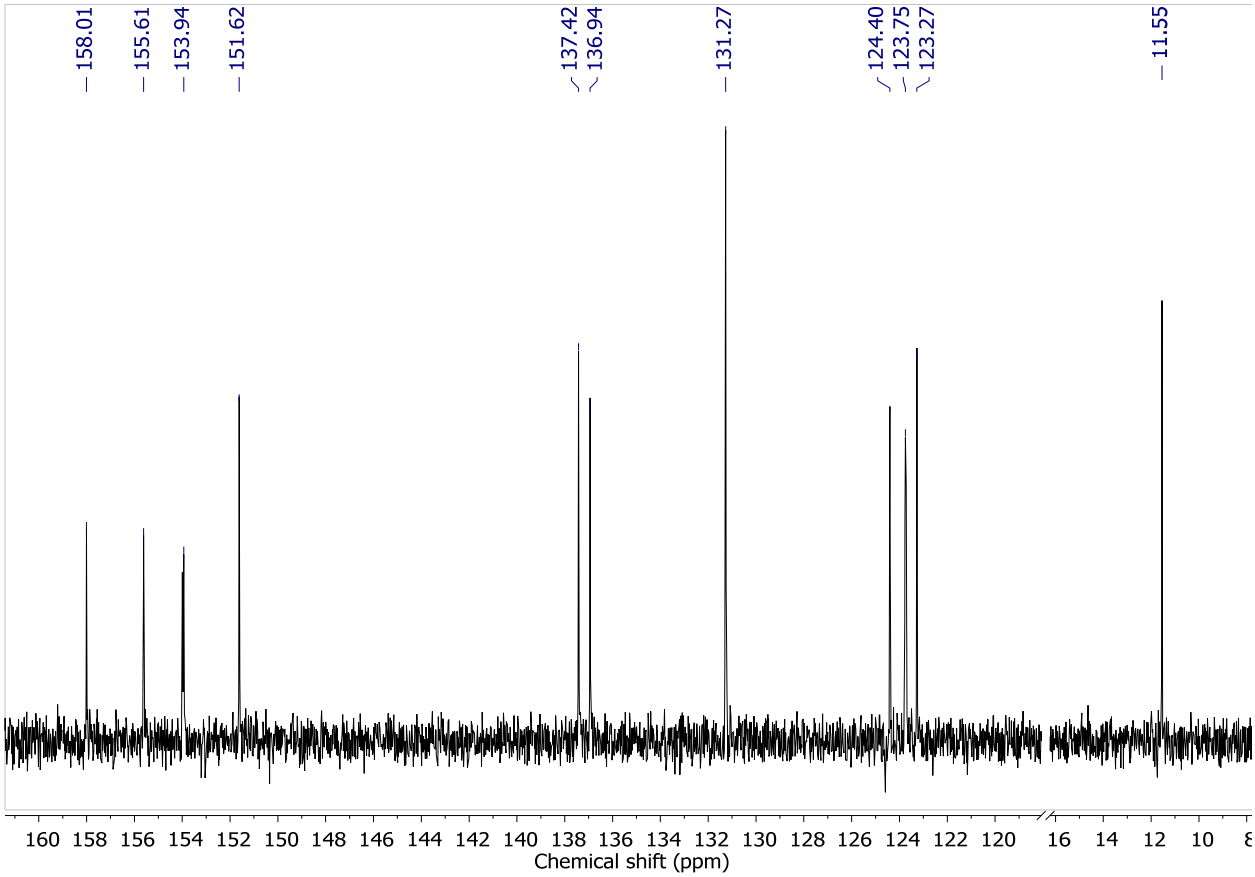

Fig. S8. ^{13}C NMR spectrum of the solution of the complex [**Fe(AcPyOx)$_3$(ZrPc)](ClO$_4$)** in CD_2Cl_2.

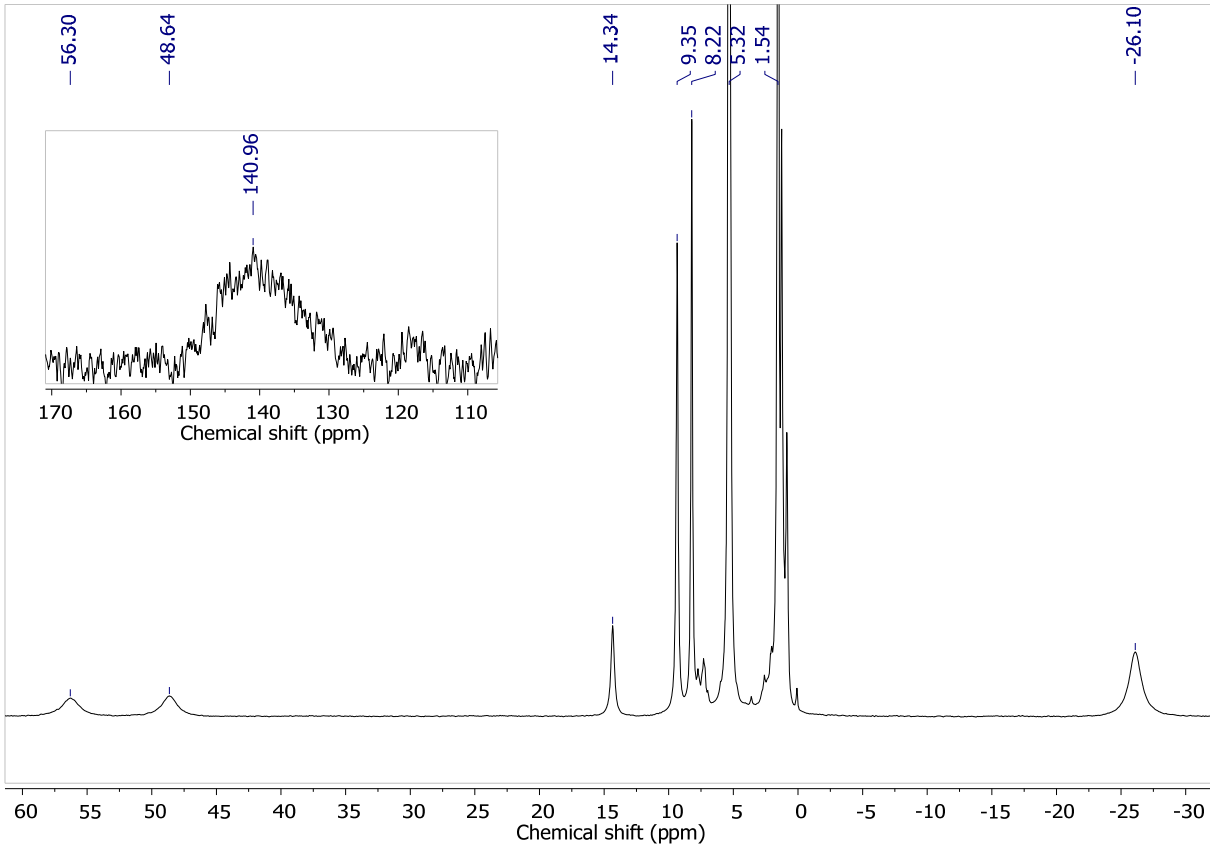

Fig. S9. ^{1}H NMR spectrum of the solution of the complex [**Ni(AcPyOx)$_3$(HfPc)](ClO$_4$)** in CD_2Cl_2.

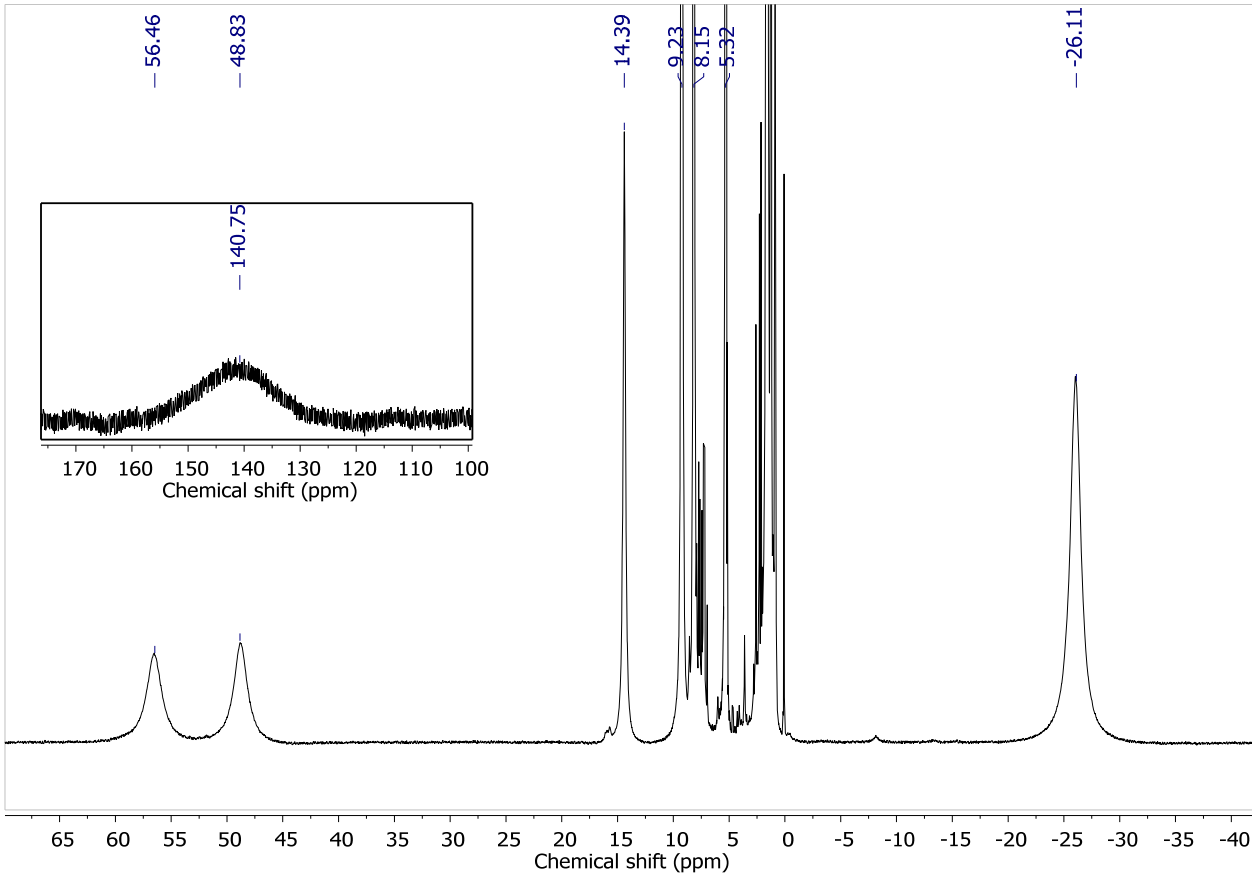

Fig. S10. ^{1}H NMR spectrum of the solution of the complex **[Ni(AcPyOx)$_3$(ZrPc)](ClO$_4$)** in CD_2Cl_2.

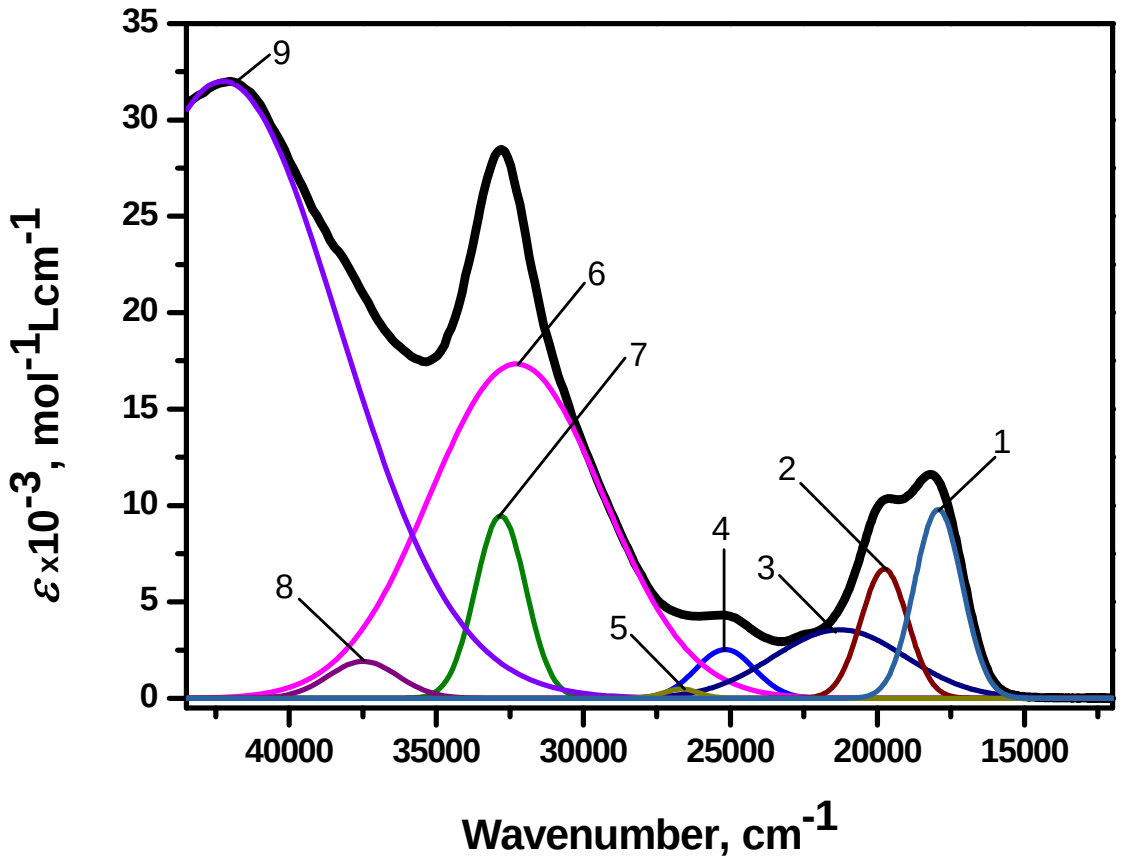

Fig. S11. UV-vis spectrum of the dichloromethane solution of the complex **[Fe(AcPyOx)$_3$(Sb(C$_2$H$_5$)$_3$)](ClO$_4$)** (in black) and its deconvoluted Gaussian components (in color).

Table S1. Gaussian Fit Parameters for the **[Fe(AcPyOx)$_3$(Sb(C$_2$H$_5$)$_3$)](ClO$_4$)**

band	E (cm^{-1})	fwhm (cm^{-1})	f_{osc} [a]
1	17928	1919	0.08598
2	19764	1869	0.05733
3	21288	5291	0.08604
4	25178	2326	0.02694
5	26680	1387	0.00306
6	32272	6951	0.55169
7	32810	2015	0.08729
8	37488	2795	0.02447
9	42264	9309	1.36381

[a]Oscillator strength (f_{osc}) = 4.3 × 10^{-9} × area under the absorption band.

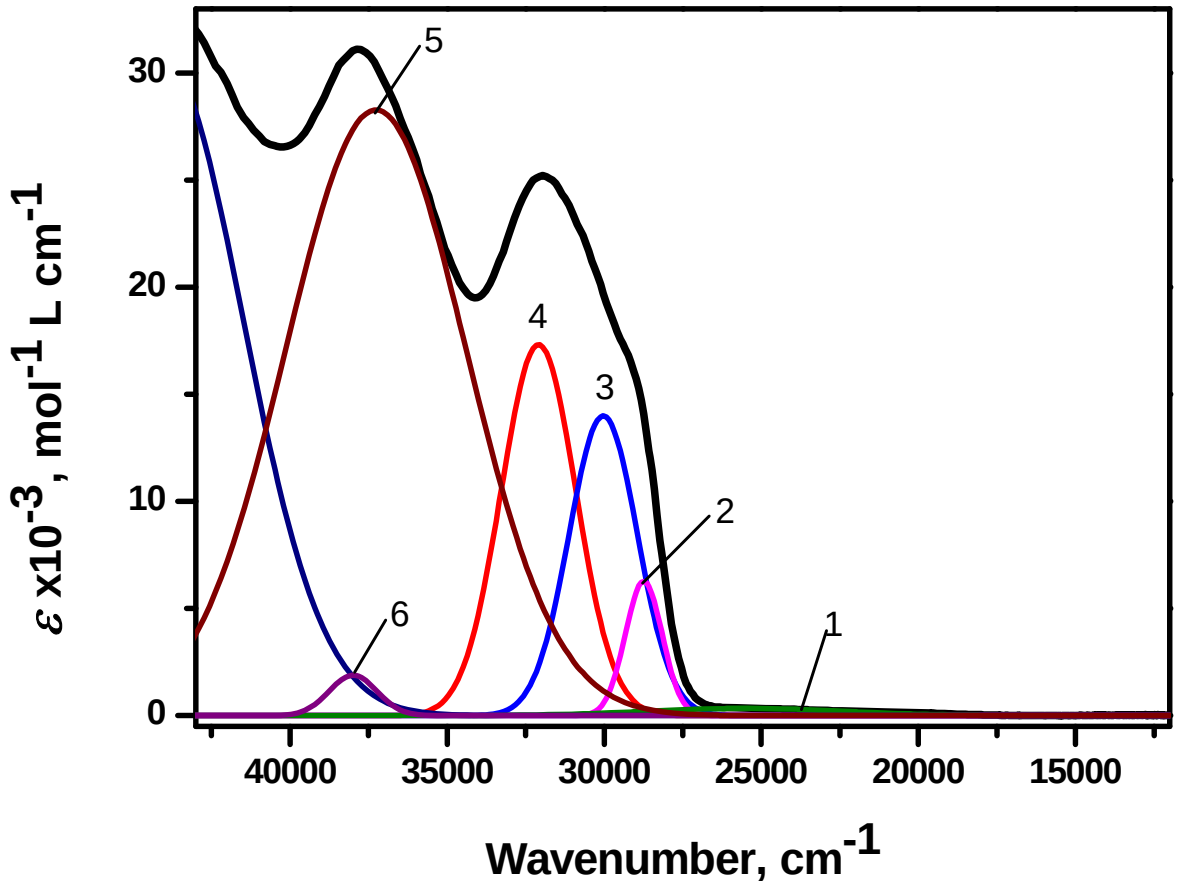

Fig. S12. UV-vis spectrum of the dichloromethane solution of the complex **[Ni(AcPyOx)$_3$(Sb(C$_2$H$_5$)$_3$)](ClO$_4$)** (in black) and its deconvoluted Gaussian components (in color).

Table S2. Gaussian Fit Parameters for the **[Ni(AcPyOx)$_3$(Sb(C$_2$H$_5$)$_3$)](ClO$_4$)**

band	E (cm^{-1})	fwhm (cm^{-1})	f_{osc} [a]
1	25523	7311	0.01136
2	28742	1385	0.03976
3	30031	2558	0.16388
4	32090	2801	0.22207
5	37268	6741	0.87280
6	37996	1784	0.01539

[a]Oscillator strength (f_{osc}) = 4.3 × 10^{-9} × area under the absorption band.

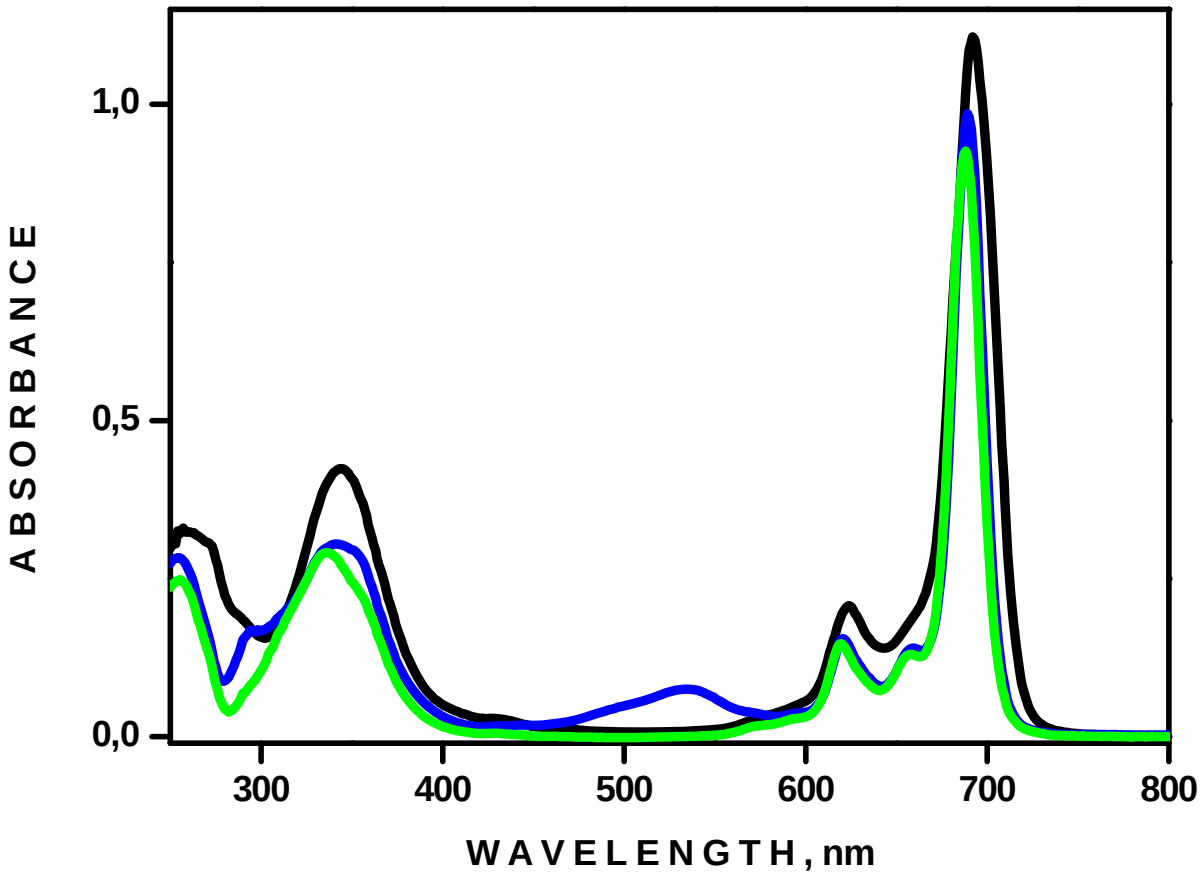

Fig. S13. UV-vis spectra of the solution of the parent phthalocyaninate **Zr(Cl_2)Pc** in DMSO (in black) and the dichloromethane solutions of its derivatives **[Fe(AcPyOx)$_3$(ZrPc)](ClO_4)** (in blue) and **[Ni(AcPyOx)$_3$(ZrPc)](ClO_4)** (in green).

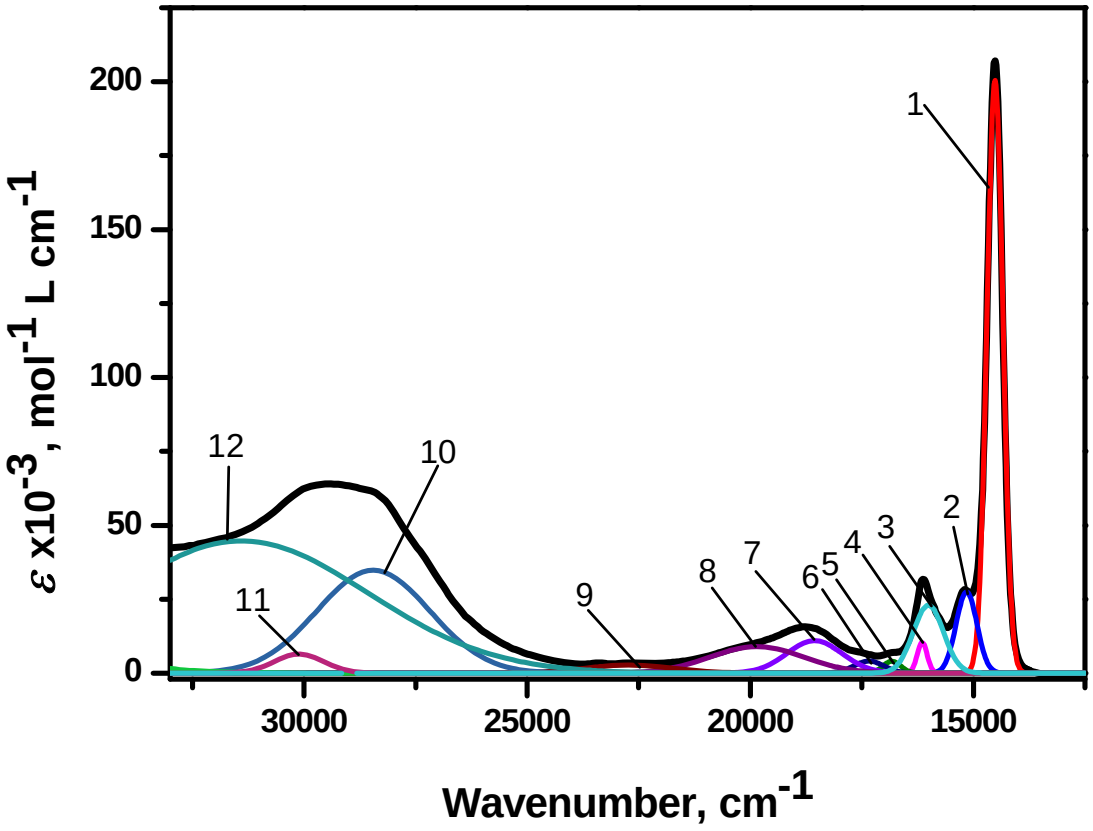

Fig. S14. UV-vis spectrum of the dichloromethane solution of the complex **[Fe(AcPyOx)$_3$(HfPc)](ClO$_4$)** (in black) and its deconvoluted Gaussian components (in color).

Table S3. Gaussian Fit Parameters for the **[Fe(AcPyOx)$_3$(HfPc)](ClO$_4$)**

band	E (cm^{-1})	fwhm (cm^{-1})	f_{osc} [a]
1	14512	412	0.37553
2	15173	687	0.0866
3	16077	609	0.08266
4	16787	426	0.00893
5	17293	845	0.01674
6	18565	1471	0.07600
7	19876	2424	0.09839
8	22706	2385	0.03015
9	25383	2019	0.02051
10	28449	2979	0.47499
11	30115	1230	0.03826
12	31403	6665	1.36387

[a]Oscillator strength (f_{osc}) = 4.3 × 10^{-9} × area under the absorption band.

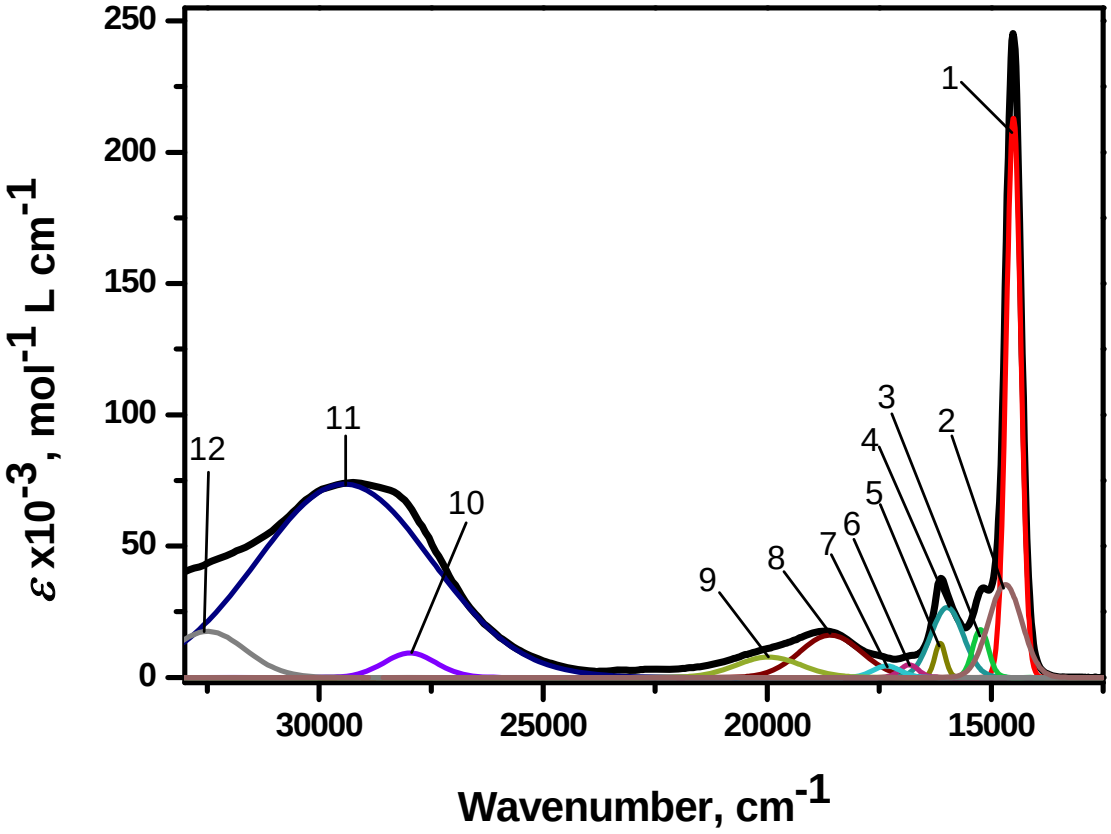

Fig. S15. UV-vis spectrum of the dichloromethane solution of the complex **[Fe(AcPyOx)$_3$(ZrPc)](ClO$_4$)** (in black) and its deconvoluted Gaussian components (in color).

Table S4. Gaussian Fit Parameters for the **[Fe(AcPyOx)$_3$(ZrPc)](ClO$_4$)**

band	E (cm^{-1})	fwhm (cm^{-1})	f_{osc} [a]
1	14503	380	0.37131
2	14687	866	0.14019
3	15238	412	0.03439
4	15985	850	0.10347
5	16140	282	0.01678
6	16834	475	0.01047
7	17336	714	0.01417
8	18587	1605	0.11840
9	19964	1700	0.06018
10	27975	1367	0.05791
11	29433	4574	1.54125
12	32486	1960	0.15706

[a]Oscillator strength (f_{osc}) = 4.3 × 10^{-9} × area under the absorption band.

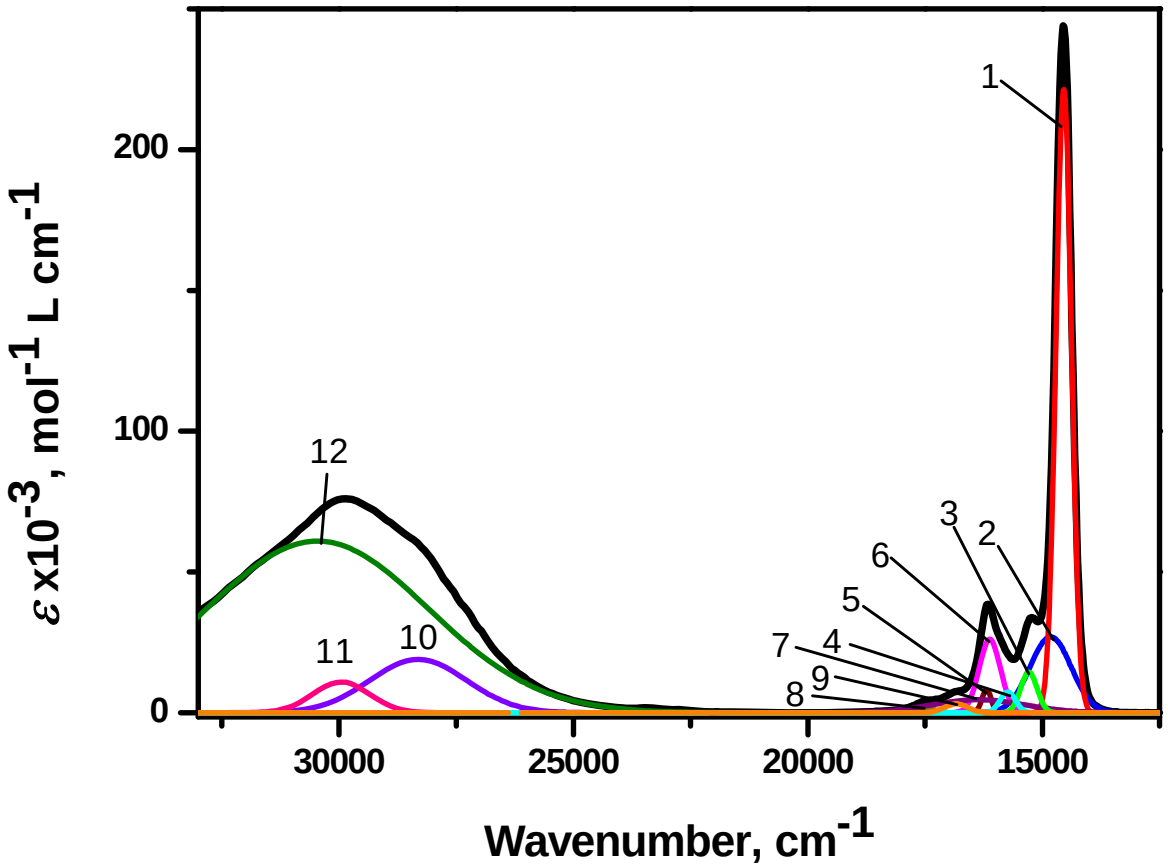

Fig. S16. UV-vis spectrum of the dichloromethane solution of the complex **[Ni(AcPyOx)$_3$(HfPc)](ClO$_4$)** (in black) and its deconvoluted Gaussian components (in color).

Table S5. Gaussian Fit Parameters for the **[Ni(AcPyOx)$_3$(HfPc)](ClO$_4$)**

band	E (cm^{-1})	fwhm (cm^{-1})	f_{osc} [a]
1	14543	385	
2	14822	1028	
3	15286	410	
4	15737	389	
5	16120	532	
6	16190	233	
7	16366	2341	
8	16836	580	
9	17490	470	
10	28310	2435	
11	29953	1421	
12	30475	5563	

[a]Oscillator strength (f_{osc}) = 4.3 × 10^{-9} × area under the absorption band.

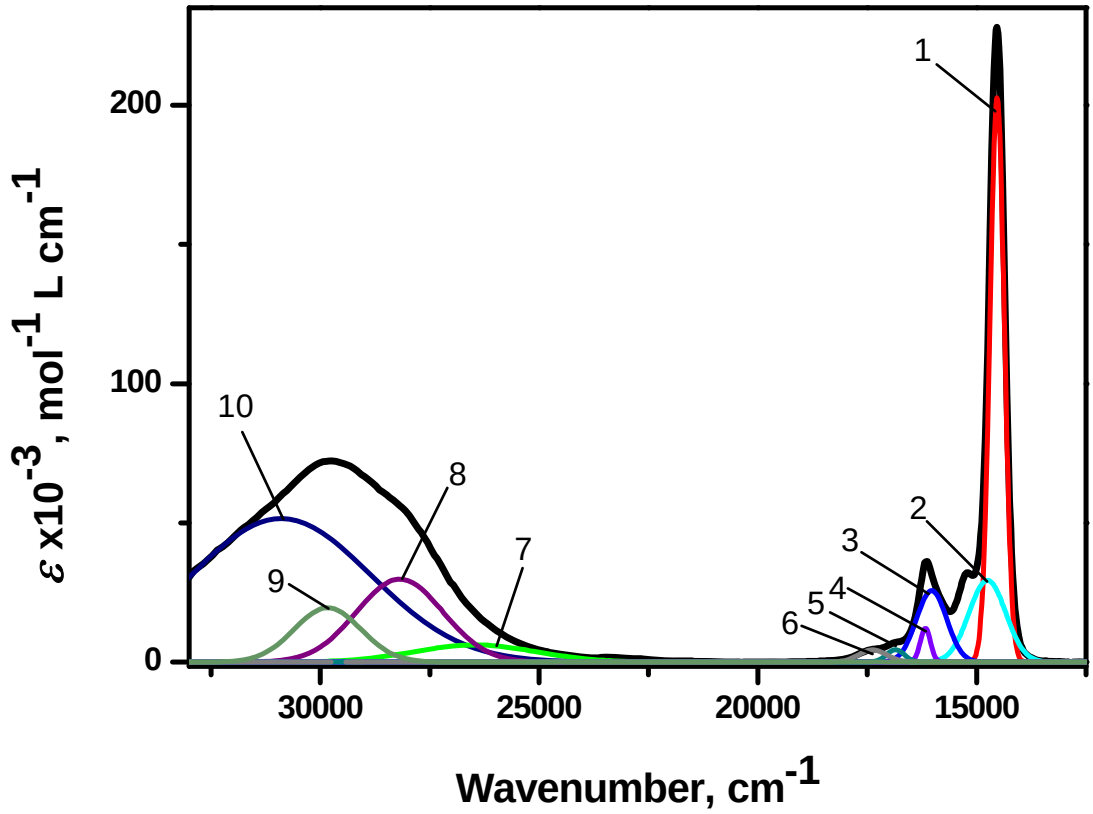

Fig. S17. UV-vis spectrum of the dichloromethane solution of the complex **[Ni(AcPyOx)$_3$(ZrPc)](ClO$_4$)** (in black) and its deconvoluted Gaussian components (in color).

Table S6. Gaussian Fit Parameters for the **[Ni(AcPyOx)$_3$(ZrPc)](ClO$_4$)**

band	E (cm^{-1})	fwhm (cm^{-1})	f_{osc} [a]
1	14532	387	0.35864
2	14753	983	0.13228
3	16030	811	0.09533
4	16172	276	0.01530
5	16857	471	0.00966
6	17375	753	0.01519
7	26463	3269	0.09239
8	28184	2323	0.31683
9	29835	1793	0.16027
10	36838	1024	0.02295

[a]Oscillator strength (f_{osc}) = 4.3 × 10^{-9} × area under the absorption band.

Table S7. Details of data collection and refinement for the complexes **[Fe(AcPyOx)$_3$(HfPc)](ClO$_4$)**, **[Fe(AcPyOx)$_3$(ZrPc)](ClO$_4$)**, **[Ni(AcPyOx)$_3$(HfPc)](ClO$_4$)**, **[Ni(AcPyOx)$_3$(ZrPc)](ClO$_4$)** and **[Ni(AcPyOx)$_3$(Sb(C$_2$H$_5$)$_3$)](ClO$_4$)**.

Complex	**[Fe(AcPyOx)$_3$(HfPc)](ClO$_4$)**	**[Fe(AcPyOx)$_3$(ZrPc)](ClO$_4$)**	**[Ni(AcPyOx)$_3$(HfPc)](ClO$_4$)**	**[Ni(AcPyOx)$_3$(ZrPc)](ClO$_4$)**	**[Ni(AcPyOx)$_3$(SbEt$_3$)]ClO$_4$**
Empirical formula	$C_{53}H_{37}ClFeHfN_{14}O_7$	$C_{53}H_{37}ClFeZrN_{14}O_7$	$C_{63}H_{48}Cl_3NiHfN_{14}O_7$	$C_{53}H_{37}ClNiZrN_{14}O_7$	$C_{27}H_{36}ClN_6NiO_7Sb$
Formula weight	1251.75	1164.48	1456.70	1167.34	772.53
Crystal system	Triclinic	Monoclinic	Monoclinic	Triclinic	Trigonal
Space group	*P-1*	*P2$_1$/n*	*P2$_1$/n*	*P-1*	*R-3*
a (Å)	12.1688(19)	12.7726(16)	16.714(2)	12.3075(16)	12.9295(6)
b (Å)	13.742(2)	12.7063(16)	19.114(2)	13.6996(18)	12.9295(6)
c (Å)	15.640(2)	29.868(4)	19.356(3)	16.041(2)	31.955(3)
α (°)	79.198(3)	90	90	76.481(3)	90
β (°)	81.175(3)	100.255(2)	108.853(3)	79.763(3)	90
γ (°)	89.104(4)	90	90	87.948(3)	120
V (Å^3)	2538.4(7)	4770.0(10)	5852.1(13)	2587.8(6)	4626.3(6)
D_{calc} (g cm^{-3})	1.638	1.622	1.653	1.498	1.664
Linear absorption, μ (cm^{-3})	24.51	6.52	23.01	6.84	16.27
F(000)	1248	2368	2924	1188	2352
$2\theta_{max}$, °	52	52	58	54	58
Reflections measured	33117	75600	68743	45611	19347
Independent reflections	9953	9372	16173	11305	2743

R_{int}	0.0795	0.1888	0.0788	0.0969	0.0518
Observed refls ($I > 2\sigma(I)$)	7030	6010	12473	7901	2327
Parameters	698	697	901	697	145
wR_2	0.1807	0.2488	0.1013	0.1487	0.1279
R_1	0.0710	0.1076	0.0486	0.0583	0.0377
Goodness-of-fit	1.002	1.558	1.067	1.019	1.015
Largest diff. peak/hole (e $Å^{-3}$)	2.945 / −0.542	3.937 / −1.379	1.340 / −1.522	1.650 / −1.066	1.764 / −1.246

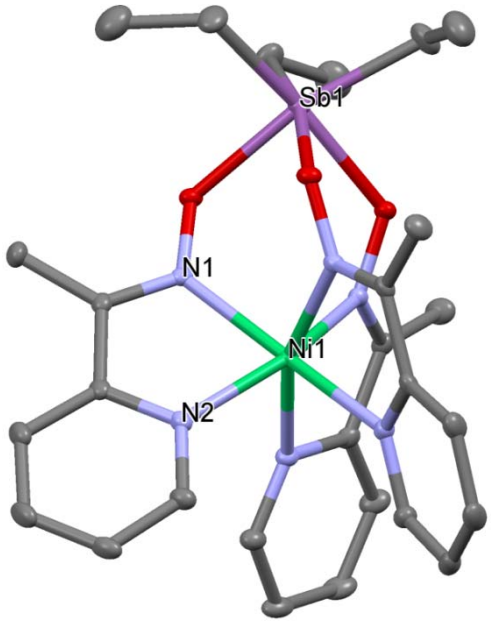

Fig. S18 General view of the complex **[Ni(AcPyOx)$_3$(SbEt$_3$)]ClO$_4$** with atoms shown as thermal ellipsoids at p=30%; hydrogen atoms and the perchlorate anion are omitted for clarity.

Table S8 Main geometrical parameters of **[Ni(AcPyOx)$_3$(SbEt$_3$)]ClO$_4$**.[a]

Parameter	Value	Parameter	Value
M–N1 (Å)	2.025(2)	N–O (Å)	1.353(3)
M–N2 (Å)	2.106(2)	Sb–O (Å)	2.146(3)
φ (°)	35.8	C=N (Å)	1.288(4)
α (°)	38.8	C–C (Å)	1.475(4)
h (Å)	2.37	N=C–C=N (°)	8.0(3)

[a] Only third of the complex is symmetry-independent in the crystal.

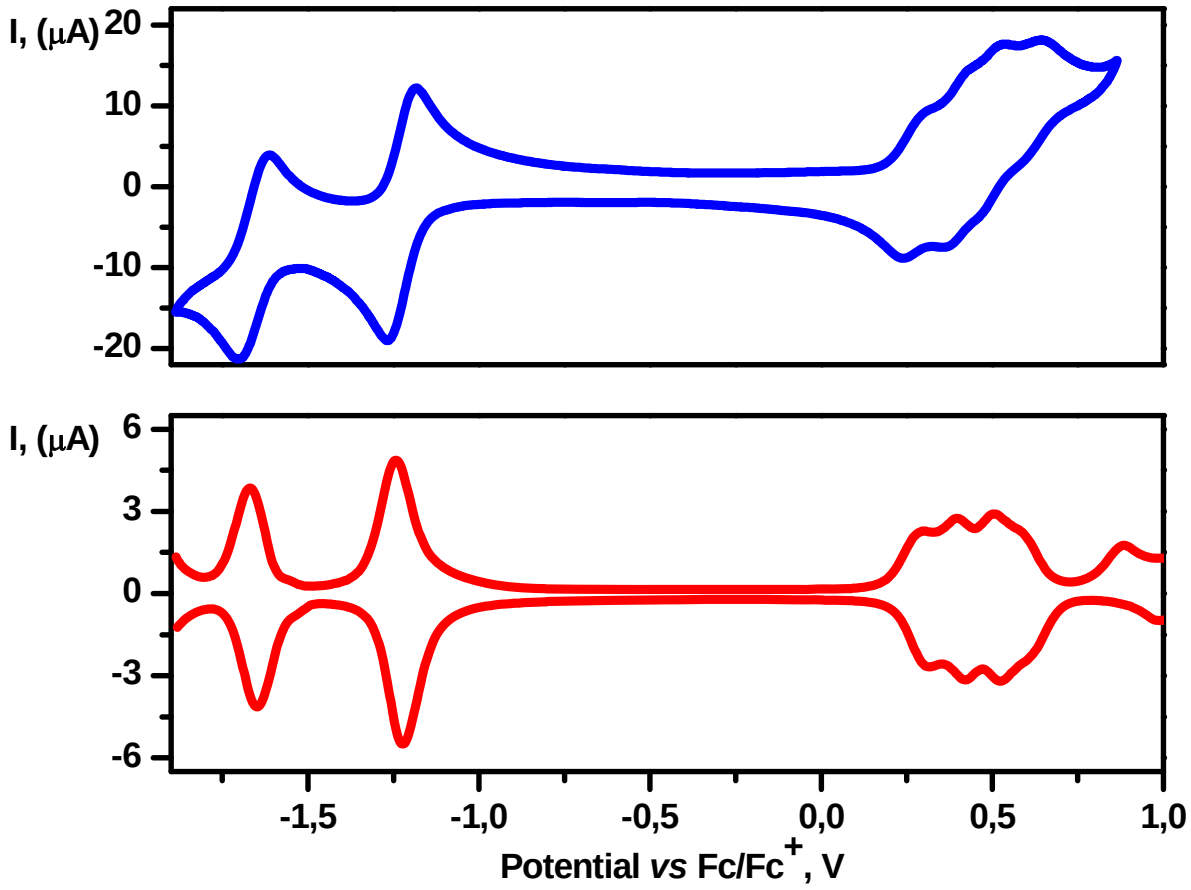

Fig. S19 Cyclic (in blue) and differential pulse (in red) voltammograms for a 0.1 mM dichloromethane solution of the complex **[Fe(AcPyOx)$_3$(HfPc)](ClO$_4$)**.